Large Elasto-Optic Effect in Epitaxial $PbTiO_3$ Films

Lan Chen,[1] Yurong Yang,[2,*] Zhigang Gui,[2] D. Sando,[3] M. Bibes,[4] X. K. Meng,[1,†] and L. Bellaiche[2]
[1]National Laboratory of Solid State Microstructures,
Collaborative Innovation Center of Advanced Microstructures,
College of Engineering and Applied Sciences, Nanjing University, Nanjing 210093, China
[2]Department of Physics and Institute for Nanoscience and Engineering,
University of Arkansas, Fayetteville, Arkansas 72701, USA
[3]School of Materials Science and Engineering, University of New South Wales,
Kensington, New South Wales 2052, Australia
[4]Unité Mixte de Physique, CNRS, Thales, Univ. Paris-Sud, Université Paris-Saclay, 91767 Palaiseau, France
(Received 11 September 2015; revised manuscript received 29 October 2015; published 30 December 2015)

First-principles calculations are performed to investigate the elasto-optic properties of four different structural phases in (001) epitaxial $PbTiO_3$ films under tensile strain: a tetragonal (T) phase and an orthorhombic (O) phase, which are the ground states for small and large strain, respectively, and two low-symmetry, monoclinic phases of Cm and Pm symmetries that have low total energy in the intermediate strain range. It is found that the refractive indices of the T and O phases respond differently to epitaxial strain, evidenced by a change of sign of their effective elasto-optic coefficients, and as a result of presently discovered correlations between refractive index, axial ratio, and magnitude of the ferroelectric polarization. The difference in refractive indices between T and O and the existence of such correlations naturally lead to large elasto-optic coefficients in the Cm and Pm states in the intermediate strain range, because Cm structurally bridges the T and O phases (via polarization rotation and a rapid change of its axial ratio) and Pm adopts a similar axial ratio and polarization magnitude to Cm. The present results therefore broaden the palette of functionalities of ferroelectric materials, and suggest new routes to generate systems with unprecedentedly large elasto-optic conversion.

DOI: 10.1103/PhysRevLett.115.267602 PACS numbers: 77.80.bn, 78.20.Ci, 78.20.hb

Ferroelectric materials have been known for several decades to exhibit large piezoelectric and dielectric responses [1,2]. Some of their other cross-coupling properties have also received considerable attention, resulting in new perspectives of using ferroelectrics in photovoltaic applications [3] and the discovery of, e.g., strong electro-optic effects [4–6], giant photo-induced strain [7], and coupling between optical fields and ferroelectric order [8,9]. One particular conversion between properties of different nature, which, to the best of our knowledge has only been studied in a few ferroelectrics (or perovskites), is the effect of strain on the refractive index [10,11], which is described by the so-called elasto-optic coefficients [12,13]. It is thus timely to ascertain whether some ferroelectrics can also exhibit large elasto-optic coefficients, an endeavor which would open up new possibilities towards applications aimed at controlling optical fields and mechano-optical transduction [13]. In particular, in view of the strong responses of their polarization to strain or applied electric field, it is appropriate to wonder if (and why) low-symmetry ferroelectric phases can generate large conversion between elastic and optical properties. Such low-symmetry phases have recently been discovered in ferroelectrics, when varying composition in some solid solutions or strain in epitaxial films, and these variations are accompanied by a rotation of the polarization [14–25].

Motivated to resolve this significant fundamental and technological issue, we have investigated the elasto-optic properties of epitaxial films of the prototypic ferroelectric material $PbTiO_3$ (PTO), through first-principles methods. An important reason for the choice of this particular system is that depending on the amount of misfit (tensile) strain they experience, these films can form (high-symmetry) tetragonal and orthorhombic states, but also low-symmetry, intermediate monoclinic phases [14,26–38]. As we describe in the following, surprises are in store for this PTO system: the monoclinic phases are predicted to possess one of the largest elasto-optic coefficients ever reported. Specifically, these coefficients are found to be about two times greater than those of lithium niobate ($LiNbO_3$), and about 30%–60% larger than that of quartz (SiO_2), the current materials of choice for the control of optical fields by acoustic effects. More detailed analysis of our computations elucidates the precise origins of this large elasto-optic transduction in PTO films. The present work thus demonstrates that, and explains why, strained ferroelectrics should be seriously considered for the design of efficient acousto-optic devices. It should also motivate further experimental work in the domain of materials optimization for application in such devices.

Here, density-functional calculations within the local density approximation (LDA) are performed, using the

Vienna *ab initio* simulation package (VASP) [39]. In order to mimic epitaxial (001) $PbTiO_3$ films, a periodic 20-atom supercell is chosen with the following lattice vectors: $\boldsymbol{a} = a_{\mathrm{IP}}(\mathbf{x}+\mathbf{y})$, $\boldsymbol{b} = a_{\mathrm{IP}}(-\mathbf{x}+\mathbf{y})$, $\boldsymbol{c} = a_{\mathrm{IP}}[\delta_1\mathbf{x} + \delta_2\mathbf{y} + (\delta_3+2)\mathbf{z}]$, where a_{IP} is the in-plane lattice constant of the substrate, and $\mathbf{x}$, $\mathbf{y}$, and $\mathbf{z}$ are unit vectors along the pseudocubic [100], [010], and [001] directions, respectively. For any given a_{IP}, the δ_1, δ_2, and δ_3 variables are relaxed, in addition to the atomic positions, to minimize the total energy within 10^{-7} eV and the Hellman-Feynman forces on each atom within 0.001 eV/Å. An energy cutoff of 600 eV and the projected augmented wave method are used [40]. A $5\times5\times3$ and an $8\times8\times6$ Monkhorst-Park k-point mesh is employed for structural relaxation and calculation of optical properties, respectively. The polarization $\mathbf{P}$ is evaluated from the product of the atomic displacements with the Born effective charges (note that we also computed the polarization from the Berry phase method [41] and found values around 10% larger). Using this approach, we have found and systematically studied four states. The first is a tetragonal (T) phase in the $P4mm$ space group that has its polarization lying along the pseudocubic [001] axis. The second state is an orthorhombic (O) phase adopting the $Ima2$ space group, characterized by a polarization oriented along the $\boldsymbol{a}$ axis with slight oxygen octahedra tilting of about 1° about the same in-plane direction. The third state is a monoclinic Cm phase, which can be considered a structural bridge between the T and O phases since its polarization can lie along any pseudocubic [uuv] direction—that is, between the pseudocubic [001] and [110] directions within the (−110) plane. Finally, the fourth state is also of monoclinic symmetry; however, its space group is Pm and its electrical polarization is rather oriented along pseudo-cubic [$u0u$] directions. All four investigated phases have previously been observed and/or predicted in epitaxial PTO films [14,28–31,42], and low-symmetry monoclinic Cm and Pm states have also been reported in $Pb(Zr,Ti)O_3$ [19,43] $Pb(Mg_{1/3}Nb_{2/3})O_3-PbTiO_3$ [20] and $Pb(Sc_{1/2}Nb_{1/2})O_3-PbTiO_3$ [21,22] solid solutions within certain Ti compositional ranges.

The imaginary part of the dielectric tensor is obtained via

$$\varepsilon''_{\alpha\beta}(\omega) = \frac{4\pi^2 e^2}{\Omega}\lim_{q\to0}\frac{1}{q^2}\sum_{c,v,\mathbf{k}} 2\omega_{\mathbf{k}}\delta(\epsilon_{c\mathbf{k}} - \epsilon_{v\mathbf{k}} - \hbar\omega) \times \langle u_{c\mathbf{k}+\mathbf{e}_\alpha q}|u_{v\mathbf{K}}\rangle\langle u_{c\mathbf{k}+e_\beta q}|u_{v\mathbf{K}}\rangle^*, \quad (1)$$

where the indices c and v refer to conduction and valence band states, respectively, $u_{c\mathbf{k}}$ is the cell-periodic part of the Bloch orbitals at the k point $\mathbf{k}$, $\mathbf{e}_\alpha$ and $\mathbf{e}_\beta$ are unit vectors along the α and β Cartesian direction, respectively [44], and the asterisk symbol denotes the complex conjugate. The real part of the dielectric tensor $\varepsilon'_{\alpha\beta}$ is then extracted through the Kramers-Kronig transformation $\varepsilon'_{\alpha\beta}(\omega) = 1 + (2/\pi)P\int_0^\infty\{[\varepsilon''_{\alpha\beta}(\omega')\omega']/(\omega'^2-\omega^2)\}d\omega'$, where P denotes the principal value. We point out also that the dielectric function thus determined takes into account local field effects in the random-phase approximation. We obtain the extinction coefficient k and refractive index n from

$$\tilde{\varepsilon}_{\alpha\beta} = \varepsilon'_{\alpha\beta} + i\varepsilon''_{\alpha\beta} = (n_{\alpha\beta} + ik_{\alpha\beta})^2. \quad (2)$$

In the following, we concentrate on energies $\hbar\omega$ smaller than the electronic band gap (experimentally known to be 3.4 eV in bulk PTO [45,46]), which implies that, as consistent with the formula above, $\varepsilon''_{\alpha\beta}(\omega)$ vanishes and the refractive index is thus simply equal to the square root of $\varepsilon'_{\alpha\beta}(\omega)$ (information about $\varepsilon''_{\alpha\beta}(\omega)$ for energies above the band gap is provided in the Supplemental Material [47]). Our first-principles computations of the refractive index of PTO within its band gap are found to be rather accurate. This is demonstrated by the prediction of an average refractive index, $(n_{11}+n_{22}+n_{33})/3$, equal to 2.81 for an energy about 40% smaller than the band gap, which compares well with the experimentally measured value of 2.67 at a wavelength of 633 nm [48].

We then compute the elasto-optic coefficient p_{ij} via

$$\Delta\left(\frac{1}{n^2}\right)_i = \sum_j p_{ij}\eta_j, \quad (3)$$

where η_j are components of the strain tensor (in Voigt notation) and $\Delta(1/n^2)_i$ is the resulting strain-induced change in the inverse of the square of the refractive index [49–51]. More precisely, we only consider here the '1' and '2' components of the strain tensor (with the 1, 2, and 3 axes being along the pseudocubic [100], [010], and [001] directions, respectively) in this formula, with $\eta_1 = \eta_2$, to reflect epitaxial growth of the film. The resulting effective elasto-optic coefficients are thus obtained from the following relations: $[1/n_1^2(\eta_1)] - [1/n_1^2(0)] = (p_{11}+p_{12})\eta_1$, $[1/n_2^2(\eta_1)] - [1/n_2^2(0)] = (p_{21}+p_{22})\eta_1$, and $[1/n_3^2(\eta_1)] - [1/n_3^2(0)] = (p_{31}+p_{32})\eta_1$. Note that for the T, O, and Cm phases of epitaxial PTO films, $n_1 = n_2 = n_o$, which is known as the *ordinary* refractive index and $n_3 = n_e$, which is termed the *extraordinary* refractive index. On the other hand, for the Pm phase of epitaxial PTO films, the x and y directions are not equivalent by symmetry (due to the polarization direction), and therefore n_1 and n_2 differ, implying that the effective $(p_{11}+p_{12})$ is different from the effective $(p_{21}+p_{22})$ in that state. We highlight here that our first-principles methods can predict elasto-optic coefficients rather accurately: additional computations performed for bulk $LiNbO_3$ (using the hexagonal setting) yield $p_{31} = 0.17$ for a photon energy being roughly halfway within its band gap. This value is in very good agreement with the corresponding experimental value of 0.18 [12].

Let us now define the strain η as the relative difference between any chosen a_{IP} and the in-plane lattice constant that provides the lowest possible value of the total energy

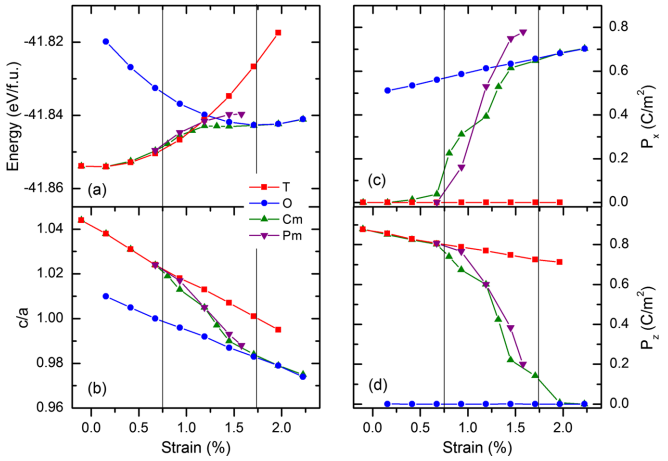

FIG. 1 (color online). Total energy (a), axial ratio (b), x component of the polarization, P_x (c), and out-of-plane component of the polarization, P_z (d), of PTO films as a function of tensile strain. Note that while the y component of the polarization P_y is equal to P_x for the O and Cm phases, it vanishes for the T and Pm phases.

of the $P4mm$ state (this in-plane constant is numerically found here to be 3.87 Å, in good agreement with the measured a lattice parameter of 3.89 Å of bulk PTO [52]). Figure 1 presents the total energy, axial ratio [which is computed as $(\delta_3 + 2)/2$], and polarization of the four investigated phases of PTO films under tensile epitaxial strain—that is, for positive η. For small tensile strain up to 1%, the tetragonal T phase possesses the lowest energy and is therefore the ground state, consistent with the fact that bulk PTO is known to adopt a $P4mm$ state below ~760 K [53]. The axial ratio of this tetragonal phase decreases from 1.04 to 1.02, while its out-of-plane polarization (P_z) reduces from 0.87 C/m^2 to 0.80 C/m^2, as η increases from 0 to 0.75%. On the other hand, in the strain window of 0.75% to 1.75%, the Cm phase first becomes a metastable low-energy state (between 0.75% and 1%) and then the ground state, with the Pm state also being close in energy. The almost energy-degenerate nature of these two phases implies that either one of them can likely be stabilized in PTO films by, e.g., playing with epitaxial strain or other effects (such as applying electric fields along specific directions and then removing them, or varying the growth conditions or thickness of the film). In this latter strain range, the T phase is metastable, and its axial ratio continues to decrease to about 1.004 while its z polarization shrinks to 0.73 C/m^2. Interestingly, the axial ratio of the Cm phase crosses unity in this strain range since it is equal to 1.022 when $\eta = 0.75\%$ and is about 0.988 for an epitaxial strain of 1.75%. Meanwhile for the Cm phase, increasing η from 0.75% to 1.75% causes the in-plane polarization $P_{x/y}$ (the x and y components of polarization are equal in this monoclinic phase) to increase from zero to 0.66 C/cm^2 and the out-of-plane polarization P_z to concomitantly decrease from 0.75 C/cm^2 to almost zero. In other words, the polarization of the Cm state continuously rotates from the out-of-plane [001] direction towards the in-plane [110] direction in this intermediate strain range. Finally, regarding the Pm monoclinic phase, Fig. 1(b) reveals that its axial ratio is qualitatively—and even quantitatively—very similar to that of the Cm phase for strain values between 0.75% to 1.75%, and Fig. 1(d) further indicates that its out-of-plane polarization rapidly decreases with increasing tensile strain. On the other hand, its in-plane polarization has only an x component (P_y always vanishes in Pm, unlike in Cm), resulting in the polarization of Pm rotating from the pseudocubic [001] to [100] directions with increasing tensile strain. We point out that it is known that the polarization of ferroelectric and multiferroic films can indeed rotate towards in-plane directions when the film is subject to tensile strain (see, e.g., Refs. [23,24,27,32,36] and references therein). Figure 1(a) also shows that Pm has a slightly higher energy than the T and Cm phases in the entire strain region extending from 0.75% to 1.75%, implying that Pm is *metastable* rather than the true ground state here. Interestingly, both Pm and Cm phases have been observed for PTO films grown on a $DyScO_3$ substrate (corresponding to a biaxial strain of 1.4%) [31], which demonstrates the accuracy and pertinence of the present simulations. Figure 1 also indicates that the orthorhombic (O) phase becomes the ground phase when η is larger than 1.75%, with an axial ratio smaller than 1 and an in-plane component of the polarization increasing from 0.91 to 0.99 C/m^2 as the strain increases from 1.75% to 2.5%.

Having described the stability regions and ferroelectric properties of the various phases, we now turn to the investigation of *elasto-optic* effects in PTO films. To that end, Fig. 2(a) presents the ordinary and extraordinary refractive indices, n_o and n_e, respectively, of the T, O, and Cm phases as a function of epitaxial strain, for an $\hbar\omega$ energy being 0.3 eV smaller than the computed band gap of bulk PTO (note that this computed band gap is equal to 1.8 eV, which, as usual with the LDA method, underestimates the experimental band gap of 3.4 eV [45,46]). Figure 2(a) also reports the in-plane n_1 and n_2 refractive indices of the Pm phase as well as the out-of-plane n_3 index at this energy. One can see from Fig. 2(a) that n_o is larger than n_e for the T phase for the range of strain explored here, while the reverse situation holds for the O phase. On the other hand, the hierarchy between n_o and n_e is found to be dependent on the strain range in the Cm phase. As a result, and as depicted in Fig. S3 of the Supplemental Material [47], the birefringence, which is simply the difference between n_e and n_o, remarkably changes sign within the Cm phase. In order to further understand these results, Fig. 2(b) displays the same data as in Fig. 2(a) but plotted as a function of the axial ratio corresponding to each selected misfit strain and phase. The data of Fig. 2(b) reveal that the

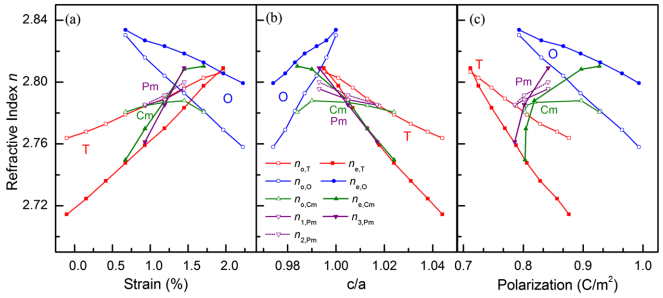

FIG. 2 (color online). Panel (a): Refractive index n of ordinary (open symbols) and extraordinary rays (filled symbols) for the T (squares), O (dots), and Cm (up triangles) phases as a function of strain for an $\hbar\omega$ energy being 0.3 eV below the computed band gap. In-plane and out-of-plane refractive indices of the Pm phase (down triangles) are also shown. Panels (b) and (c): as for panel (a) but as a function of the axial ratio and magnitude of the polarization, respectively.

hierarchy between the magnitude of n_o and n_e is strongly correlated to the axial ratio for the T, O, and Cm phases: to a very good approximation, the ordinary refractive index is larger (smaller) than the extraordinary one if the axial ratio is larger (smaller) than unity for these three phases (note that a similar relation between indices of refraction and axial ratio, and the resulting hierarchy between indices of refraction, are also found for the Pm phase, but when comparing the averaged in-plane index, $(n_1 + n_2)/2$, with that of the out-of-plane, n_3). As a result, and as evidenced in Fig. 2(a), n_o and n_e reverse their mutual hierarchy for epitaxial strain close to 1.25% in the monoclinic Cm state.

It is important to realize that both the ordinary and extraordinary refractive indices respond very differently to epitaxial strain in the T *versus* O phases: they linearly increase with strain in the tetragonal state, while the converse is true in the orthorhombic phase. This difference in behavior can be traced back to the polarization: as evidenced in Fig. 2(c), both n_o and n_e decrease with the magnitude of the overall polarization in both the T and O phases, but this polarization decreases with tensile strain in the T phase while it increases with η in the O phase, as demonstrated in Figs. 1(c) and 1(d) (note that the Supplemental Material [47] provides additional information about the relation between refractive indices and Cartesian components of polarization). Moreover, the striking difference between the strain dependence of the refractive indices in the T versus O phases, along with the fact that the monoclinic Cm state continuously structurally bridges the T and O phases, result in the refractive indices of Cm adopting *nonmonotonic* behaviors with strain. In particular, for the Cm state for η close to 1.2%, n_o is almost independent of strain while n_e is much more sensitive to η than in the T and O phases. More precisely, this insensitivity of n_o to strain for η near 1.2% in the Cm phase originates from the fact that the ordinary refractive index of the T phase for, e.g., $\eta = 1.0\%$ is very similar to that of the O state for, e.g., $\eta = 1.5\%$ [see Fig. 2(a)] and that Cm is the bridge between the T and O states in that strain range. Similarly, n_e of the Cm phase responds considerably to epitaxial strain near 1.2% because the extraordinary refractive index of the T phase for, e.g., $\eta = 0.75\%$ is relatively much smaller (because of their rather different axial ratio) than that of the O state for, e.g., $\eta = 1.75\%$. Therefore, n_e of Cm has to change abruptly with strain in order to bridge these two limiting extraordinary refractive indices [note that the Pm state exhibits n_1 and n_3 refractive indices that are very similar to n_o and n_e of the Cm phase, respectively, as shown in Fig. 2(a)].

TABLE I. Elasto-optic coefficients for the four studied phases of epitaxial (001) PTO films under a tensile strain of 1.2%, for an $\hbar\omega$ energy being 0.3 eV below the computed band gap. The number in parentheses corresponds to $(p_{21} + p_{22})/2$ of the Pm phase, which, due to symmetry and unlike in the T, O, and Cm phases, differs from $(p_{11} + p_{12})/2$. Note that $p_{31} = p_{32}$ in the T, O, and Cm states, therefore making $[(p_{31} + p_{32})/2] = p_{31}$ in these three phases.

Phase	T	O	Pm	Cm
$(p_{11} + p_{12})/2$	−0.10	0.20	−0.09 (−0.13)	−0.04
$(p_{31} + p_{32})/2$	−0.22	0.10	−0.43	−0.35

As revealed in Table I, the unusual strain-dependent behavior of n_o and n_e in the monoclinic states has a strong influence on the elasto-optic properties near $\eta = 1.2\%$: the Cm state has an effective average $\frac{1}{2}(p_{11} + p_{12})$ coefficient (associated with n_o) that merely vanishes, while the effective elasto-optic coefficient $\frac{1}{2}(p_{31} + p_{32})$ of Cm and Pm (related to n_e in Cm and n_3 in Pm) has twice the magnitude of that of the T phase and is 4 times larger than that of the O phase. In fact, to the best of our knowledge, these $\frac{1}{2}(p_{31} + p_{32})$ parameters are the largest elasto-optic coefficients found in any material. For instance, they are about twice as large as the elasto-optic coefficient of lithium niobate, for which $p_{31} = 0.18$, and 30%–60% bigger than that of quartz ($p_{31} = 0.29$) [12]. Most importantly, we find that these elevated values of $\frac{1}{2}(p_{31} + p_{32})$ in the Cm and Pm phases of PTO films are predicted to occur for any epitaxial strain ranging between 1.0% and 1.5%; i.e., they are not only valid for the selected strain of 1.2% associated with Table I. This suggests that epitaxial growth of PTO on, e.g., a $DyScO_3$ substrate (corresponding to $\eta = 1.4\%$), should lead to large elasto-optic coefficients in such films. Note that the possibility of having large elasto-optic couplings in ferroelectrics was previously proposed in Ref. [54], but for bulk systems (namely, $KNbO_3$ and $BaTiO_3$) and using a simple theoretical approach with parameters determined from some measurements.

In summary, first-principle computations were performed to investigate structural and elasto-optic properties of epitaxial $PbTiO_3$ films under tensile strain, for four

different crystallographic states. In particular, it was found that the tetragonal and orthorhombic states have rather different values and strain-dependent behavior for their extraordinary refractive index, a result of the fact that (i) the axial ratio of the T state is larger than 1 while it is smaller than unity in the O state, and (ii) that the refractive indices decrease linearly with the magnitude of the polarization in both states—with the polarization magnitude increasing with epitaxial strain in the O phase while it decreases in the T phase. An important consequence of the differences between the n_e of the tetragonal and orthorhombic states is that the low-symmetry Cm phase possesses large elasto-optic coefficients over a particular strain range, arising from the fact that it structurally bridges these T and O phases in that range. The other studied monoclinic state, the Pm phase, also exhibits a large elasto-optic response, mostly because it exhibits an axial ratio and polarization magnitude which both depend on strain in a very similar fashion to those of the Cm state in the aforementioned strain range.

The present study therefore provides a new route towards the engineering of large elasto-optic properties, namely, to search for low-symmetry phases possessing a rapid evolution of their axial ratio and Cartesian components of the polarization. Such a rapid evolution can occur in epitaxial ferroelectric films upon variation of the magnitude of epitaxial strain [14,15]. Other possibilities also exist, for instance, playing with the composition in the so-called morphotropic phase boundaries of certain solid solutions [16,55] or with hydrostatic pressure [56–58]. We therefore hope that the current Letter will lead to a deeper understanding of, and possibilities to optimize, elasto-optic properties, and that the results will pave the way to the further application of ferroelectrics in photonics and acousto-optic devices. It will also be interesting to determine in future studies if (multi)domain configurations [59] can also yield a large elasto-optic coupling.

This work is supported by ONR Grant No. N00014-12-1-1034, DARPA Grant No. HR0011-15-2-0038 (MATRIX program) and the Jiangsu Planned Projects for Postdoctoral Research Funds (under Grant No. 1302043B). We also acknowledge a challenge grant from DOD allowing us the access of supercomputers, and the Arkansas High Performance Computer Center at the University of Arkansas.

*yyrwater@uark.edu
†mengxk@nju.edu.cn

[1] M. E. Lines and A. M. Glass, *Principles and Applications of Ferroelectrics and Related Materials* (Oxford University Press, New York, 1977).
[2] J. Scott, Science **315**, 954 (2007).
[3] I. Grinberg, D. V. West, M. Torres, G. Gou, D. M. Stein, L. Wu, G. Chen, E. M. Gallo, A. R. Akbashev, P. K. Davies *et al.*, Nature (London) **503**, 509 (2013).
[4] S. Abel, T. Stöferle, C. Marchiori, C. Rossel, M. D. Rossell, R. Erni, D. Caimi, M. Sousa, A. Chelnokov, B. J. Offrein *et al.*, Nat. Commun. **4**, 1671 (2013).
[5] T. Miyamoto, H. Yada, H. Yamakawa, and H. Okamoto, Nat. Commun. **4**, 2586 (2013).
[6] D. Sando, P. Hermet, J. Allibe, J. Bourderionnet, S. Fusil, C. Carrétéro, E. Jacquet, J. C. Mage, D. Dolfi, A. Barthélémy *et al.*, Phys. Rev. B **89**, 195106 (2014).
[7] M. Lejman, G. Vaudel, I. C. Infante, P. Gemeiner, V. E. Gusev, B. Dkhil, and P. Ruello, Nat. Commun. **5**, 4301 (2014).
[8] Y. M. Sheu, S. A. Trugman, L. Yan, Q. X. Jia, A. J. Taylor, and R. P. Prasankumar, Nat. Commun. **5**, 5832 (2014).
[9] F. Rubio-Marcos, A. Del Campo, P. Marchet, and J. F. Fernández, Nat. Commun. **6**, 6594 (2015).
[10] A. Dejneka, M. Tyunina, J. Narkilahti, J. Levoska, D. Chvostova, L. Jastrabik, and V. A. Trepakov, Phys. Solid State **52**, 2082 (2010).
[11] D. Imbrenda, D. Yang, H. Wang, A. R. Akbashev, B. A. Davidson, X. Wu, X. Xi, and J. E. Spanier, arXiv:1510.01709.
[12] I. C. Chang, in *Handbook of Optics*, edited by M. Bass (McGraw-Hill, New York, 1995), Vol. 2, p. 1.
[13] D. Royer and E. Dieulesaint, *Elastic Waves in Solids II: Generation, Acousto-Optic Interaction, Applications* (Springer Science & Business Media, New York, 2000), Vol. 2.
[14] G. Catalan, A. Lubk, A. H. G. Vlooswijk, E. Snoeck, C. Magen, A. Janssens, G. Rispens, G. Rijnders, D. H. A. Blank, and B. Noheda, Nat. Mater. **10**, 963 (2011).
[15] R. J. Zeches, M. D. Rossell, J. X. Zhang, A. J. Hatt, Q. He, C.-H. Yang, A. Kumar, C. H. Wang, A. Melville, C. Adamo *et al.*, Science **326**, 977 (2009).
[16] Y. M. Jin, Y. U. Wang, A. G. Khachaturyan, J. F. Li, and D. Viehland, Phys. Rev. Lett. **91**, 197601 (2003).
[17] K. A. Schönau, L. A. Schmitt, M. Knapp, H. Fuess, R.-A. Eichel, H. Kungl, and M. J. Hoffmann, Phys. Rev. B **75**, 184117 (2007).
[18] H. Fu and R. E. Cohen, Nature (London) **403**, 281 (2000).
[19] B. Noheda, D. E. Cox, G. Shirane, J. A. Gonzalo, L. E. Cross, and S.-E. Park, Appl. Phys. Lett. **74**, 2059 (1999).
[20] B. Noheda, D. E. Cox, G. Shirane, J. Gao, and Z. G. Ye, Phys. Rev. B **66**, 054104 (2002).
[21] R. Haumont, A. Al-Barakaty, B. Dkhil, J. M. Kiat, and L. Bellaiche, Phys. Rev. B **71**, 104106 (2005).
[22] R. Haumont, B. Dkhil, J. M. Kiat, A. Al-Barakaty, H. Dammak, and L. Bellaiche, Phys. Rev. B **68**, 014114 (2003).
[23] Z. Gui, S. Prosandeev, and L. Bellaiche, Phys. Rev. B **84**, 214112 (2011).
[24] O. Diéguez, K. M. Rabe, and D. Vanderbilt, Phys. Rev. B **72**, 144101 (2005).
[25] L. Bellaiche, A. García, and D. Vanderbilt, Phys. Rev. Lett. **84**, 5427 (2000).
[26] G. Sheng, J. X. Zhang, Y. L. Li, S. Choudhury, Q. X. Jia, Z. K. Liu, and L. Q. Chen, J. Appl. Phys. **104**, 054105 (2008).
[27] N. A. Pertsev, a. G. Zembilgotov, and a. K. Tagantsev, Phys. Rev. Lett. **80**, 1988 (1998).
[28] M. J. Highland, D. D. Fong, G. B. Stephenson, T. T. Fister, P. H. Fuoss, S. K. Streiffer, C. Thompson, M. I. Richard, and J. A. Eastman, Appl. Phys. Lett. **104**, 132901 (2014).
[29] O. Nesterov, S. Matzen, C. Magen, A. H. G. Vlooswijk, G. Catalan, and B. Noheda, Appl. Phys. Lett. **103**, 142901 (2013).

[30] S. Matzen, O. Nesterov, G. Rispens, J. A. Heuver, M. Biegalski, H. M. Christen, and B. Noheda, Nat. Commun. **5**, 4415 (2014).
[31] G. Catalan, A. Janssens, G. Rispens, S. Csiszar, O. Seeck, G. Rijnders, D. H. A. Blank, and B. Noheda, Phys. Rev. Lett. **96**, 127602 (2006).
[32] J. L. Blok, D. H. A. Blank, B. A, G. Rijnders, K. M. Rabe, and D. Vanderbilt, Phys. Rev. B **84**, 205413 (2011).
[33] H. Sharma, J. Kreisel, and Ph. Ghosez, Phys. Rev. B **90**, 214102 (2014).
[34] G. Sághi-Szabó, R. E. Cohen, and H. Krakauer, Phys. Rev. B **59**, 12771 (1999).
[35] B. Meyer and D. Vanderbilt, Phys. Rev. B **65**, 104111 (2002).
[36] Y. Yang, W. Ren, M. Stengel, X. H. Yan, and L. Bellaiche, Phys. Rev. Lett. **109**, 057602 (2012).
[37] T. Nishimatsu, M. Iwamoto, Y. Kawazoe, and U. V. Waghmare, Phys. Rev. B **82**, 134106 (2010).
[38] Y. Yang, M. Stengel, W. Ren, X. H. Yan, and L. Bellaiche, Phys. Rev. B **86**, 144114 (2012).
[39] G. Kresse and D. Joubert, Phys. Rev. B **59**, 1758 (1999).
[40] P. E. Blöchl, Phys. Rev. B **50**, 17953 (1994).
[41] R. D. King-Smith and D. Vanderbilt, Phys. Rev. B **47**, 1651 (1993).
[42] A. H. G. Vlooswijk, B. Noheda, G. Catalan, A. Janssens, B. Barcones, G. Rijnders, D. H. A. Blank, S. Venkatesan, B. Kooi, and J. T. M. De Hosson, Appl. Phys. Lett. **91**, 112901 (2007).
[43] A. Sani, B. Noheda, I. A. Kornev, L. Bellaiche, P. Bouvier, and J. Kreisel, Phys. Rev. B **69**, 020105 (2004).
[44] M. Gajdoš, K. Hummer, G. Kresse, J. Furthmüller, and F. Bechstedt, Phys. Rev. B **73**, 045112 (2006).
[45] C. H. Peng, J.-F. Chang, and S. B. Desu, Mater. Res. Soc. Symp. Proc. **243**, 21 (1991).
[46] M. P. Moret, M. A. C. Devillers, K. Wörhoff, and P. K. Larsen, J. Appl. Phys. **92**, 468 (2002).
[47] See Supplemental Material at http://link.aps.org/supplemental/10.1103/PhysRevLett.115.267602 for additional details on predicted optical and electronic properties of PTO epitaxial films.
[48] C. M. Foster, G.-R. Bai, R. Csencsits, J. Vetrone, R. Jammy, L. A. Wills, E. Carr, and J. Amano, J. Appl. Phys. **81**, 2349 (1997).
[49] S. Pezzagna, J. Brault, M. Leroux, J. Massies, and M. De Micheli, J. Appl. Phys. **103**, 123112 (2008).
[50] M. Zgonik, P. Bernasconi, M. Duelli, R. Schlesser, P. Gunter, M. H. Garrett, D. Rytz, Y. Zhu, and X. Wu, Phys. Rev. B **50**, 5941 (1994).
[51] H. Koc, H. Ozisik, E. Deligöz, A. M. Mamedov, and E. Ozbay, J. Mol. Model. **20**, 2180 (2014).
[52] G. Shirane, S. Hoshino, and K. Suzuki, Phys. Rev. **80**, 1105 (1950).
[53] R. E. Cohen, Nature (London) **358**, 136 (1992).
[54] P. Bernasconi, M. Zgonik, and P. Günter, J. Appl. Phys. **78**, 2651 (1995).
[55] T. T. A. Lummen, Y. Gu, J. Wang, S. Lei, F. Xue, A. Kumar, A. T. Barnes, E. Barnes, S. Denev, A. Belianinov *et al.*, Nat. Commun. **5**, 3172 (2014).
[56] M. Ahart, M. Somayazulu, R. E. Cohen, P. Ganesh, P. Dera, H.-k. Mao, R. J. Hemley, Y. Ren, P. Liermann, and Z. Wu, Nature (London) **451**, 545 (2008).
[57] J. Rouquette, J. Haines, V. Bornand, M. Pintard, P. Papet, W. G. Marshall, and S. Hull, Phys. Rev. B **71**, 024112 (2005).
[58] Z. Wu and R. E. Cohen, Phys. Rev. Lett. **95**, 037601 (2005).
[59] A. Grünebohm, M. Marathe, and C. Ederer, Appl. Phys. Lett. **107**, 102901 (2015).